microbiology research

MDPI

Article

Evaluation of a Bivalent *Hexon-L1* and *Fiber-2* Subunit Vaccine Candidate Against Homologous Fowl Adenovirus Serotype 4 Challenge in Chickens

Xiaoran Chu [1], Kaili Wang [1], Vincenzo Cuteri [1,2,*], Cheng Liu [1], Yubao Li [3] and Zhenshu Si [1,*]

[1] College of Agriculture and Biology, Liaocheng University, Liaocheng 252000, China; wkl202218@163.com (K.W.); liucheng@lcu.edu.cn (C.L.)
[2] School of Biosciences and Veterinary Medicine, University of Camerino, 62024 Matelica, Italy
[3] School of Pharmaceutical Sciences and Food Engineering, Liaocheng University, Liaocheng 252000, China; liyubao@lcu.edu.cn
* Correspondence: vincenzo.cuteri@unicam.it (V.C.); dckszs@163.com (Z.S.); Tel.: +39-073-740-4001 (V.C.); +86-139-6301-8715 (Z.S.)

Abstract

Fowl adenovirus serotype 4 (FAdV-4) is the major causative agent of hydropericardium-hepatitis syndrome (HHS), a disease responsible for considerable economic losses in poultry production. Although inactivated and live-attenuated vaccines reduce mortality, continued outbreaks highlight the need to optimize vaccination strategies. To address these limitations, we developed and evaluated a bivalent subunit vaccine composed of recombinant hexon-L1 and fiber-2 proteins, two major antigenic determinants associated with neutralization and pathogenicity. The proteins were expressed in *Escherichia coli*, purified under native conditions, confirmed for purity and antigenicity, and emulsified into a water-in-oil formulation. Chickens were immunized with either 10 µg or 20 µg doses, boosted after 14 days, and challenged with the homologous virulent FAdV-4 strain SDLC202009. The 20 µg dose conferred complete survival, eliminated histopathological lesions, prevented viral detection in tissues by PCR and immunohistochemistry, and fully blocked viral shedding. Similarly, the 10 µg dose induced a good protection with only minor pathological differences compared to the group treated with 20 µg. These results demonstrate that a bivalent *hexon-L1* and *fiber-2* subunit formulation elicits strong, dose-dependent humoral and tissue-level protection against homologous FAdV-4 challenge under the conditions tested. The experimental design did not include a monovalent *fiber-2* comparator; therefore, conclusions regarding the relative contribution of each antigen are not drawn.

Keywords: FAdV-4; subunit vaccine; *hexon-L1*; *fiber-2*; chicken

Check for updates

Academic Editors: Beniamino T. Cenci-Goga and Seyed Ali Ghorashi

Received: 11 December 2025
Revised: 24 February 2026
Accepted: 24 February 2026
Published: 26 February 2026

1. Introduction

1.1. Epidemiology and Economic Impact of Fowl Adenovirus Serotype 4

Fowl adenovirus serotype 4 (FAdV-4), a member of the genus *Aviadenovirus* (family *Adenoviridae*), is the primary etiological agent of hepatitis-hydropericardium syndrome (HHS), a disease responsible for severe economic losses in the global poultry industry. Recently, the International Committee on Taxonomy of Viruses (ICTV) introduced Latinized binomial names for fowl adenoviruses, including *Aviadenovirus ventriculi*, *A. quintum*, *A. hydropericardii*, *A. gallinae*, and *A. hepatitidis* [1]. To maintain consistency with the existing literature, the traditional classification into species A–E is retained in this study, with FAdV-4 corresponding to *A. hydropericardii*.

Fowl adenoviruses are further classified into twelve serotypes (FAdV-1 to -8a and FAdV-8b to -11), originally defined by serum neutralization tests and later supported by molecular genotyping [2]. Among these, FAdV-4 has received particular attention due to the emergence of hypervirulent strains that have caused widespread outbreaks with high mortality rates since 2015, especially in China [3,4]. FDvA-4 virus infection can progress to Hemorrhagic-Hyperinflammatory Syndrome (HHS), a severe, often fatal, multi-system illness. The virus replicates massively in the liver, causing severe hepatocellular damage and necrosis. This leads to acute hepatic insufficiency, hypoalbuminemia, increased vascular permeability, and the resultant effusions (hydropericardium, ascites). Death is typically due to acute heart failure or liver failure [5].

FAdV-4 strains are broadly categorized into two distinct pathotypes based on their virulence in chickens (Supplementary Table S1). Classical strains, such as the prototype ON1 (GenBank: GU188428), typically cause subclinical infections or mild disease with low mortality (<10%) under experimental conditions [3]. In contrast, the hypervirulent strains that have emerged since 2015—exemplified by isolates such as SDLC202009 (OP484855), SD1601 (KU361926), and JSJ13 (KM096544)—are associated with mortality rates reaching 30–100% in broiler flocks [3,4,6]. Genomic comparisons have identified critical molecular determinants distinguishing these pathotypes, with most amino acid substitutions in hypervirulent strains clustering within the *fiber-2* and *hexon* genes [3,7,8]. These differences include specific mutations in the *fiber-2* knob domain, which may enhance viral attachment and replication efficiency in target tissues [7,8]. The emergence and widespread circulation of these hypervirulent strains underscore the need for vaccines capable of inducing robust protective immunity.

The substantial and ongoing economic burden associated with these outbreaks underscores the urgent need for effective and reliable prophylactic strategies, as continued circulation of FAdV-4 has been reported despite vaccine availability [4,9].

1.2. Virological Features and Antigenic Targets for Vaccine Development

FAdV-4 is a non-enveloped, double-stranded DNA virus with a genome of approximately 45 kb encoding both structural and non-structural proteins [6]. Among the structural proteins, *hexon* and *fiber-2* play critical roles in viral pathogenicity and host interaction, making them prime targets for vaccine development [10]. *Hexon* is the most abundant capsid protein and is highly immunogenic following adenovirus infection, containing regions associated with virus neutralization and serotype-specific immune responses [11]. In particular, the *hexon-L1* loop harbors group- and type-specific antigenic determinants that are dominant targets of neutralizing antibodies [12].

The fiber proteins are responsible for viral attachment to host cell receptors. While fiber-1 has shown inconsistent results as an immunization antigen, *fiber-2* has been consistently identified as a key virulence determinant in FAdV-4 infections and elicits strong neutralizing antibody responses [13]. Notably, amino acid variations in *fiber-2* have been strongly associated with increased pathogenicity, reinforcing its relevance as a vaccine antigen [7]. Targeting *fiber-2* therefore represents a rational strategy to counteract hypervirulent FAdV-4 strains [14]. By contrast, the penton protein is involved in viral internalization but remains less well characterized in terms of its immunogenic potential. Although *fiber-1* can induce neutralizing antibodies through its knob and shaft domains, its protective efficacy remains variable and requires further investigation [15].

1.3. Limitations of Current Vaccines and Rationale for a Bivalent Subunit Strategy

Since 2015, severe outbreaks of HHS have been frequently reported in China [16], and despite the availability of vaccines, the disease continues to circulate. Surveillance conducted in Shandong Province in 2022 revealed FAdV-4 positivity in 60% (12/20) of poultry farms and 56.8% (25/44) of clinical samples (unpublished data). These findings highlight the persistent circulation of FAdV-4 and the lack of fully effective control measures. Previous studies have reported that inactivated vaccines may show variable efficacy against heterologous strains, while live-attenuated vaccines carry inherent biosafety considerations, including potential reversion to virulence and environmental persistence [4,17,18]. Subunit vaccines offer a safer and genetically defined alternative, as they eliminate the introduction of viral genomic material while allowing targeted immune responses.

Previous studies have demonstrated that subunit vaccines based on capsid proteins can confer protection against FAdV-4. In particular, *fiber-2*-based vaccines have achieved the most consistent protective outcomes against HHS. Conversely, vaccination with fiber-1 has yielded highly variable results, with inconsistent survival rates following virulent challenge [19,20]. Although *hexon* is highly immunogenic, vaccination with recombinant *hexon-L1* alone has failed to confer complete protection, regardless of antigen dose, despite inducing detectable ELISA antibody responses [19–21]. These observations suggest that while *hexon* contributes to immunogenicity, it may not be sufficient as a standalone protective antigen, highlighting the need for alternative or combined antigenic approaches.

1.4. Aim of the Present Study

Given the complementary roles of *hexon* and *fiber-2* in viral antigenicity and pathogenicity, a bivalent subunit vaccine incorporating both antigens represents a feasible and rational strategy for FAdV-4 vaccine development. Such an approach aims to combine two major antigenic determinants associated with protection and virulence, potentially enhancing the breadth and consistency of the immune response. However, experimental data evaluating the protective efficacy of a *hexon-L1* and *fiber-2* bivalent formulation against virulent FAdV-4 challenge remain limited.

In this study, we describe the production, formulation, and in vivo evaluation of a bivalent *hexon-L1* and *fiber-2* subunit vaccine in SPF chickens, with particular emphasis on survival, pathological outcomes, viral tissue distribution, and virus shedding following challenge. This work seeks to address a critical gap in FAdV-4 vaccine research by providing experimental evidence supporting the feasibility of a bivalent subunit vaccine strategy.

2. Materials and Methods

2.1. Virus and Primers

The virulent FAdV-4 strain SDLC202009 (GenBank: OP484855), previously isolated from clinical liver specimens of laying hens with HHS in Liaocheng, Shandong Province, was used as the source of genetic material [6].

Gene-specific primers for the *hexon-L1* and *fiber-2* genes were designed based on the SDLC202009 sequence using Primer Premier 5.0 software, incorporating appropriate restriction enzyme sites at the 5′ and 3′ ends (Table 1). All primers were synthesized by Beijing Tsingke Biotech Co., Ltd. (Beijing China).

Table 1. Primer list.

Gene	Primer Sequences	Annealing Temperature	Fragment Size
Hexon-L1	F:5′-ATAGGATCCATGGTCCTGGACATGGGGTC-3′ R:5′-CATAAGCTTCTCGGTATTCCGGTCGGGC-3′	53 °C	690 bp
Fiber-2	F:5′-ATAGATATCATGCTCCGGGCCCCT-3′ R:5′-AATAAGCTTTTACGGGAGGGAGGCC-3′	56.8 °C	1440 bp

The enzyme cleavage site is underlined. GGATCC is the *Bam HI* enzyme cleavage site; AAGCTT is the *HindIII* enzyme cleavage site; GATATC is the *EcoR V* enzyme cleavage site.

2.2. Animal, Ethics, Husbandry and Challenge Experiments

2.2.1. Housing Isolation and Cross-Contamination Risk Control

Housing Facilities: All experimental animals were housed in independent negative-pressure isolators.

Group Isolation: Each experimental group (including different immunization groups, challenge groups, and control groups) utilized separate isolators, achieving complete physical isolation. Sufficient distance was maintained between isolators, and all procedures (feeding, watering, observation, challenge) followed strict biosecurity protocols, effectively eliminating risks of contact and cross-contamination between groups via airborne particles, dust, or personnel handling.

2.2.2. Standardized Environmental Conditions Management

Housing environments were strictly controlled to eliminate potential environmental influences on immune responses.

Temperature: Initial temperature was 34 °C (simulating chick brooding requirements), then reduced by 2 °C weekly until maintained within a comfortable ambient range. This protocol follows standard broiler/SPF chicken husbandry guidelines.

Humidity: Relative humidity was maintained at 38% ± 5%.

Lighting: A 12 h light/12 h dark photoperiod was provided.

Feed and Water: All animals had ad libitum access to antibiotic-free, complete compound feed from the same batch and autoclave-sterilized drinking water.

2.2.3. Challenge Test Execution

During inoculation, animals were handled in biosafety cabinets, strictly separated by group, using dedicated instruments to prevent accidental virus transmission between groups.

Thirty Specific Pathogen-Free (SPF) seven-day-old chickens, hatched from SPF eggs (supplied by Spifree Poultry Technology Co., Ltd., Jinan, China), were used for the vaccination and challenge experiments. All animal procedures were approved by the Research Ethics Committee of Liaocheng University (Ethics Approval Code: 2022092001; Date: 20 September 2022) and were conducted in strict accordance with the "Guidelines for the Care and Use of Laboratory Animals" issued by the Ministry of Science and Technology of the People's Republic of China.

Prior to their use, chickens were confirmed to be free of FAdV-4 antibodies via ELISA, ensuring a naive immunological state suitable for vaccine efficacy assessment.

2.3. Amplification of Hexon-L1 and Fiber-2 Genes

The *hexon-L1* and *fiber-2* genes were amplified by PCR using SDLC202009 genomic DNA as the template and their respective primer pairs. The PCR protocol was as follows: initial denaturation at 94 °C for 5 min; 30 cycles of denaturation at 94 °C for 30 s, annealing for 30 s, and extension at 72 °C for 90 s; followed by a final extension at 72 °C for 10 min. The annealing temperature was optimized to 53 °C for *hexon-L1* and 56.8 °C for *fiber-2*. The DNA fragments of the expected size were excised and purified using the BBI EZ-10 Gel Extraction Kit (Sangon Biotech Co., Ltd., Shanghai, China), then subjected to Sanger sequencing to confirm their identity and ensure the absence of mutations.

2.4. Preparation of the Cloning Vector and Double Digestion

The purified *hexon-L1* and *fiber-2* PCR products, as well as the *pET-32a(+)* expression plasmid, were subjected to double restriction enzyme digestion (Tiangen Biochemical Technology Co., Ltd., Beijing, China). The digestion reactions were assembled according to the manufacturer's instructions. The digested insert (*hexon-L1/fibe-r2*) and vector (*pET-32a*) fragments were then purified. Subsequently, the digested *hexon-L1* and *fiber-2* fragments were ligated into the linearized *pET-32a* plasmid using T4 DNA ligase to construct the recombinant expression vectors, *pET-32a-hexon-L1* and *pET-32a-fiber-2* [22]. These recombinant plasmids were then transformed into competent *E. coli* cells for amplification and subsequent protein expression, a standard procedure for producing recombinant proteins [23].

2.5. Ligation and Transformation

The gel-purified inserts and linearized *pET-32a* vector were ligated using the TaKaRa DNA Ligation Kit Ver.2.1 (TaKaRa Bio Co., Ltd., Beijing, China). The ligation mixture was incubated at 4 °C overnight and 10 µL of the ligation product was used to transform 100 µL of chemically competent *E. coli* DH5α cells via heat-shock (42 °C for 90 s). The transformed cells were reactivated in 900 µL of Luria–Bertani (LB) broth at 37 °C for 45 min with shaking at 180 rpm. Successful transformants, identified by their ampicillin resistance, were then screened for the presence of the desired plasmid constructs via colony PCR and subsequent plasmid extraction and restriction enzyme analysis to confirm correct gene insertion and orientation.

2.6. Screening of Recombinant Clones

Six putative recombinant colonies were randomly selected and screened by colony PCR. Positive clones were inoculated into LB liquid medium containing ampicillin. Glycerol stocks (50% v/v final concentration) of positive cultures were prepared and stored at −80 °C. Plasmid DNA was extracted from the remaining culture using the TiGen Plasmid Mini Prep Kit and sent to Sangon Biotech Co, Ltd., (Shanghai, China) for Sanger sequencing to confirm the integrity of the inserted genes.

2.7. Construction of the Expression Vector

The verified recombinant plasmids (*pET-32a-hexon-L1* and *pET-32a-fiber-2*) were transformed into chemically competent *E. coli* Rosetta (DE3) cells for protein expression. Positive transformants were again confirmed by colony PCR and sequencing.

2.8. Optimization of Recombinant Protein Expression

A single positive colony for each construct was used to inoculate a small-scale culture. When the culture optical density at 600 nm (OD_{600}) reached approximately 0.6, protein expression was induced by adding Isopropyl β-D-1-thiogalactopyranoside (IPTG). To determine the optimal expression conditions, induction was tested at different temperatures (16 °C, 28 °C, 37 °C), IPTG concentrations (0.008, 0.08, 0.8 mM), and induction durations (4, 16, 24 h). A non-induced culture served as a control. After induction, the cells were harvested by centrifugation (5500× g, 20 min, 4 °C), resuspended in PBS containing 1 mM Phenylmethylsulphonyl Fluoride (PMSF), and lysed by sonication on ice. The soluble

https://doi.org/10.3390/microbiolres17030048

(supernatant) and insoluble (pellet) fractions were separated by centrifugation and analyzed by 12% SDS-PAGE.

2.9. Large-Scale Expression and Purification

Recombinant proteins were expressed in large-scale cultures under the optimal conditions determined in the previous section. The cell pellets from these cultures were lysed by sonication. The *hexon-L1* and *fiber-2* proteins, containing a C-terminal *6xHis-tag*, were purified from the soluble fraction under native conditions using a Ni-NTA affinity chromatography kit (Kangwei Century Biotechnology Co., Ltd., Beijing, China) according to the manufacturer's protocol. The bound proteins were washed with binding buffer containing increasing concentrations of imidazole (50, 70, 80, 100 mM) and eluted with binding buffer containing 200 mM imidazole. The eluted proteins were refolded using a stepwise dialysis against PBS with decreasing concentrations of urea (from 6 M to 0 M). The refolded proteins were then concentrated using polyethylene glycol (PEG) 10,000, quantified, aliquoted, and stored at −80 °C. Purity (>90%) was confirmed by SDS-PAGE followed by Coomassie blue staining and densitometry; antigenicity was validated via Western blotting using anti-FAdV-4 convalescent serum. Endotoxins were quantified using LAL assays and maintained under 1 EU/mg.

2.10. Vaccine Formulation and Quality Control

The bivalent subunit vaccine was formulated as a water-in-oil emulsion. The aqueous phase was prepared by mixing the purified *hexon-L1* and *fiber-2* proteins at a 1:1 mass ratio, with the final concentration of both antigens adjusted to 40 μg per mL. Tween-80 was added as an emulsifier at a ratio of 24:1 (aqueous phase:emulsifier). The oil phase was obtained by adding the standard white oil adjuvant (Marcol™ 52, Mobil, HarbourFront, Singapore). The vaccine emulsion was prepared by slowly adding the aqueous phase to the oil phase at a ratio of 1:2.5 (aqueous:oil) under continuous high shear mixing for 30–60 min. The physical properties of the vaccine emulsion were assessed by visual inspection (viscous, milky-white appearance) and by evaluating its stability in water with the "drop test". For the sterility test, the vaccine was inoculated into Thioglycolate Medium (for aerobes/anaerobes) and Soybean-Casein Digest Medium (for fungi/aerobes) and incubate at 20–25 °C for 14 days and at 30–35 °C for 14 days, observing periodically for turbidity. Additionally, the consistency and particle size distribution of the emulsion were analyzed to ensure uniform dispersion of antigens, thereby contributing to consistent immunogenicity.

2.11. Protective Efficacy of Vaccines

2.11.1. Animals, Immunization, and Challenge on SPF Chickens

Thirty SPF seven-day-old chicks were randomly divided into three groups, with 10 chickens in each group. Group 1 and Group 2 were immunized with 0.5 mL, containing 10 μg and 20 μg of antigens respectively, injected intramuscularly into the leg; the Control Group was injected with an equal amount of saline solution. After two weeks, a second inoculation was performed to create a booster effect and strengthen immunity. Two weeks after the second immunization, 300 μL of viral solution (virulent FAdV-4 filed strain SDLC202009, approximately $10^{4.67}$ EID_{50}) was injected intramuscularly into the leg, and the mortality of the chicks was then verified. The clinical signs and body weight of the surviving chicks were monitored daily for an additional 14-day post-challenge to evaluate overall protective efficacy. Post-mortem examinations were conducted on all deceased challenged animals to assess gross pathological changes and microscopic lesions in target organs.

2.11.2. Postmortem Examination and Detection of Viral Distribution in Tissues and Organs

All dead chickens underwent post-mortem examination to observe and document pathological changes in each organ and then evaluate them according to classification criteria (Table 2).

Table 2. Postmortem classification criteria.

No evident lesions	0 points
Mild lesions	1–3 points
Moderate lesions	4–6 points
Severe lesions	7–10 points

Note: all scores were assigned by the same personnel.

Using these criteria, the average lesion score was calculated for each organ considered.

Some organ fragments, including brain, heart, lungs, liver, kidneys, and pancreas, were homogenized. After centrifugation, the supernatant was collected and viral genomic DNA was extracted using the Edel Virus Genomic DNA Rapid Extraction Kit (Aidlab Biotechnologies Co., Ltd., Beijing, China), following the manufacturer's instructions. Finally, PCR was performed to determine the presence of the virus.

2.11.3. Histopathological and Immunohistochemistry Examinations

To prepare the histopathological specimens, the heart, liver, kidneys and pancreas of the deceased chickens were fixed in 4% paraformaldehyde for 24 h. Based on established knowledge of FAdV-4 organ tropism in hydropericardium-hepatitis syndrome, the heart, liver, kidneys, and pancreas were selected as primary target organs for histopathological examination [5,6,24,25]. Previous investigations have consistently identified these organs as sites of viral replication and characteristic pathological lesions [5,6,26].

Subsequently, sections were prepared, subjected to hematoxylin and eosin (HE) staining, then examined and photographed under a microscope. For quantitative analysis of histopathological changes, specific scoring criteria [26] were applied to assess the severity of lesions in each organ, providing an objective measure of vaccine efficacy against tissue damage. Further, immunohistochemical staining was performed on these tissues using a primary antibody specific for *fowl adenovirus serotype 4* antigens to detect viral presence and distribution at a cellular level [27,28].

2.11.4. Amplification of the Hexon Gene

The collected tissue samples undergo viral DNA extraction, followed by PCR amplification using primers *H1* and *H2*. This PCR product was then subjected to gel electrophoresis for visualization and confirmation of the amplified genes, providing molecular evidence of FAdV-4 presence within the collected samples.

2.11.5. Virus Shedding

At 3, 5, 7 and 14 days post-infection (dpi), cloacal and oral swabs were collected at random from 5 chickens of each group, control and immunized, using sterile cotton swabs. The swabs were immersed in centrifuge tubes containing 1 mL of PBS, penicillin and streptomycin. After centrifugation viral DNA was extracted from the supernatant. PCR amplification detected the FAdV genes, with an annealing temperature of 53 °C for *hexon-L1* and 56.8 °C for *fiber-2*.

2.11.6. Serological Test

Serum samples were collected at 7, 21, and 35 days of age, corresponding respectively to the time points prior to primary immunization, two weeks after the primary immunization but before the booster, and two weeks after booster immunization but before challenge, from five randomly selected and marked chickens from each group. To verify changes in antibody levels, sera were analyzed using the Shanghai Enzyme-Linked Bio Poultry Adenovirus Antibody Detection ELISA kit (Mibio Co., Ltd., Shanghai, China); the plates were read using a spectrophotometer with OD at 450 nm. A standard curve was plotted with the standard sample concentration on the x-axis and the OD value on the y-axis. The concentration of each sample was calculated based on the corresponding OD value.

2.11.7. Statistical Analysis

Statistical analysis and graphical representation of data were performed using GraphPad Prism 6.02 software. Lesion scores and titers were analyzed using Kruskal–Wallis tests with Dunn's post hoc correction. Mortality differences were evaluated via Fisher's exact test, with a p-value of <0.05 considered statistically significant for all analyses.

2.12. Control Materials, Animals, and Procedures

To ensure the validity, specificity, and reproducibility of the experimental results, a comprehensive set of control materials, animal groups, and procedural controls were implemented throughout this study. These controls are detailed below.

2.12.1. Control Animals and Housing

A dedicated control animal group was integral to the experimental design. Thirty Specific Pathogen Free (SPF) seven-day-old chickens were randomly allocated, with ten chickens assigned to the Control Group. This group received an intramuscular injection of 0.5 mL of sterile physiological saline (0.9% NaCl) at the time of primary and booster immunizations for the vaccinated groups. All control animals were housed under identical conditions as the vaccinated groups: within separate, dedicated negative-pressure isolators to ensure complete physical and airborne isolation from immunized chickens. Environmental parameters (temperature, humidity, photoperiod), feed (antibiotic-free complete compound feed), and water (autoclave-sterilized) were standardized and identical for all groups. Prior to enrollment, all chickens in the control group were confirmed to be seronegative for FAdV-4 antibodies via ELISA, establishing a naive immunological baseline.

2.12.2. Control Materials

The following control materials were used at various stages of the study:

Negative Control for Immunization: Sterile physiological saline (0.9% NaCl) was used as the inoculum for the animal Control Group.

Vector Control for Molecular Cloning: The empty *pET-32a(+)* expression plasmid was used in parallel during cloning procedures to distinguish background transformation from successful recombinant plasmid uptake.

Expression Control for Recombinant Protein: For each small- and large-scale protein expression experiment, a parallel culture of *E. coli* Rosetta (DE3) cells transformed with the empty *pET-32a(+)* vector was processed identically (including IPTG induction). Lysates from this culture served as a negative control in SDS-PAGE and Western blot analyses to confirm the specific expression of the recombinant *hexon-L1* and *fiber-2* proteins.

Adjuvant Control for Vaccine Formulation: During vaccine formulation development, an emulsion containing all vaccine components (oil phase, emulsifier) but lacking the

https://doi.org/10.3390/microbiolres17030048

recombinant antigens was prepared and subjected to the same quality control tests (sterility, stability) to rule out non-specific effects of the adjuvant system.

Negative Control Sera: For serological (ELISA) and immunological (Western blot) assays, serum samples collected from SPF chickens prior to immunization (Day 0) were used as negative controls. For immunohistochemistry, serum from a non-immunized, FAdV-4-naive chicken was used as a primary antibody negative control.

Positive Control Sera: Anti-FAdV-4 convalescent serum, obtained from chickens that had recovered from a natural FAdV-4 infection, was used as a positive control in Western blotting to confirm the antigenicity of the purified recombinant proteins.

2.12.3. Control Procedures

The following control procedures were systematically applied:

Sterility Controls: All media, buffers, and the final vaccine formulation were subjected to sterility testing by inoculation into Thioglycolate Medium and Soybean-Casein Digest Medium. Uninoculated media were incubated alongside test samples as negative sterility controls.

Molecular Biology Controls:

PCR Controls: Each PCR run included a no-template control (NTC) containing all reaction components except DNA to detect contamination of reagents, and a positive control using plasmid DNA or genomic DNA from the FAdV-4 SDLC202009 strain to confirm reaction efficacy.

Enzyme Digestion Controls: Undigested plasmid and single-enzyme digests were analyzed alongside double-digested products during recombinant plasmid construction to verify complete digestion and correct fragment sizes.

Sequencing Controls: Sanger sequencing of cloned genes included analysis of the original viral DNA sequence as a reference for comparison.

Protein Analysis Controls:

SDS-PAGE: Pre-stained protein molecular weight markers were included on every gel.

Western Blot: Membranes were probed with pre-immune (negative control) serum and anti-FAdV-4 convalescent (positive control) serum in parallel with experimental samples.

Animal Experiment Controls:

Sham-immunization: The Control Group received saline injections following the same schedule, volume, and route as the vaccinated groups.

Challenge Control: All groups, including the saline-injected Control Group, were challenged with the virulent FAdV-4 strain SDLC202009 under identical conditions, establishing the baseline pathogenicity and mortality (100% in this study).

Handling and Biosafety Controls: During all animal procedures (feeding, inoculation, sample collection), dedicated instruments and biosafety cabinets were used for each group. The order of handling always proceeded from control animals to vaccinated animals to prevent accidental cross-contamination.

Histopathological and Immunohistochemical Controls:

For immunohistochemistry (IHC), tissue sections from the challenge control group were processed with the omission of the primary antibody (replaced with dilution buffer or negative control serum) to assess non-specific binding of the detection system.

Known positive tissue sections from FAdV-4-infected birds (not part of the main experiment) were used as positive controls for IHC staining in each batch.

Statistical Analysis Controls: The data from the saline-injected Control Group served as the baseline comparator for all statistical analyses of survival, lesion scores, viral load, shedding, and antibody titers in the vaccinated groups. The use of this concurrent control group accounts for variability in the challenge stock and environmental conditions.

The implementation of these layered controls was designed to rigorously attribute observed effects specifically to the experimental vaccine and to ensure the reliability and interpretability of all generated data.

3. Results

3.1. Hexon-L1 and Fiber-2 Genes Amplification

After extracting DNA from virus-containing tissue, PCR amplification was performed using *hexon-L1* and *fiber-2* primers. The results showed that the amplified bands matched to the size of the target fragment (Figure S1). The successful amplification and size verification of these genes confirmed the presence of the viral genetic material and served as a foundational step for further molecular characterization and vaccine development.

3.2. PCR Identification of Recombinant Plasmid

The selected pure colonies containing the *hexon-L1* and *fiber-2* genes were subjected to PCR. All selected colonies tested positive indicating that both genes were successfully ligated into the *pET32a* vector (Figures S2 and S3). Subsequently, sequencing confirmed the accurate insertion and orientation of these target genes within the recombinant plasmids, ensuring their fidelity for subsequent protein expression.

3.3. Identification of Recombinant Plasmid Expression Vectors

Through double restriction enzyme digestion of the plasmid, it was confirmed that both genes were successfully inserted into the plasmid (Figure S4). This was evidenced by the observation of distinct bands corresponding to the expected sizes of the *hexon-L1* and *fiber-2* gene inserts following electrophoresis of the digested products, confirming the integrity of the recombinant constructs.

3.4. Expression of the Recombinant Plasmid

SDS-PAGE electrophoresis analysis revealed that both recombinant proteins were highly expressed in bacterial pellets. *E. coli* Rosetta strains containing recombinant plasmids *pET32a-hexon-L1* and *pET32a-fiber-2* were cultured under varying IPTG concentrations, induction times, and temperature conditions. The recombinant *hexon-L1* protein exhibited a molecular weight of 43.23 kDa, with optimal induction conditions at 37 °C and an IPTG concentration of 0.008 mM (Figure S5). The recombinant *fiber-2* protein had a molecular weight of 70.51 kDa, with optimal induction conditions at 37 °C and an IPTG concentration of 0.5 mM (Figures S6 and S7).

3.5. Purification and Quantification of the Recombinant Protein

The recombinant *hexon-L1* protein of 43.23 kDa was eluted using 70 mM imidazole binding buffer. The recombinant *fiber-2* protein of 70.51 kDa was eluted using 200 mM imidazole binding buffer (Figure S8). SDS-PAGE analysis confirmed the main band as the target protein, with a minor band below potentially representing degradation or truncation products, which are common in recombinant protein preparations.

The quantification of the three proteins was performed using the Bradford method, obtaining a final concentration of 0.389 mg/mL for the recombinant *hexon-L1* protein and 0.4 mg/mL for the *fiber-2* protein.

3.6. Characterization of a Two-Component Subunit Vaccine

The prepared subunit vaccine is a white viscous liquid. When poured into a Petri dish filled with water, the vaccine does not spread. In stability tests, no stratification occurred at the bottom of the tube after centrifugation at 4000 *rpm* for 15 min. In sterility tests, no

https://doi.org/10.3390/microbiolres17030048

bacterial/fungal growth was observed after incubation at 20–25 °C and at 30–35 °C for 14 days.

3.7. Protective Efficacy of Vaccines

3.7.1. Mortality of Chickens

The chickens remained normal for the first three days post-challenge. On the fourth day, only in the control group, abnormalities began to appear, manifesting as poor appetite, ruffled feathers, and lethargy, followed by mortality. The mortality rate reached 60%. On the fifth day, all chickens in the control group had died, while no deaths were recorded in either of the immunized groups. A Kaplan–Meier survival curve clearly illustrates these outcomes, showing 100% survival in both vaccinated groups versus 0% in the control group by day 5 post-challenge (Figure 1).

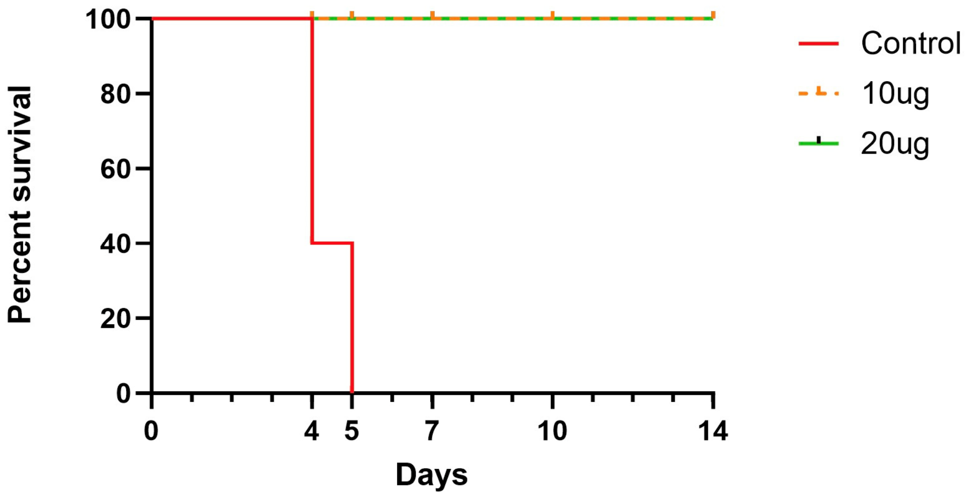

Figure 1. Survival of chickens following challenge with virulent FAdV-4. Kaplan–Meier survival curves of SPF chickens immunized with the bivalent *hexon-L1* and *fiber-2* subunit vaccine (10 μg or 20 μg per dose) and challenged with a virulent FAdV-4 strain two weeks after booster immunization. The control group received saline only. All birds in the control group succumbed to infection by 5 days post-challenge, whereas 100% survival was observed in both vaccinated groups throughout the 14-day observation period, demonstrating effective protection conferred by vaccination.

3.7.2. Effect of Vaccine Immunization on Pathological Changes

In the control group post-mortem examination revealed different degrees of pericardial effusion, the liver exhibited varying degrees of jaundice with hemorrhagic spots, the kidneys were enlarged and appeared mottled due to urate crystal deposition, the spleen was enlarged with hemorrhagic spots. In contrast, post-mortem examination of both the immunized group revealed only a few cases with minimal pericardial effusion, hepatic jaundice, and petechiae on the spleen and kidneys. Most chickens showed no significant pathological changes (Figure 2). Histopathological analysis further corroborated these gross observations, demonstrating reduced cellular necrosis and inflammation in the liver, kidney, and spleen tissues of vaccinated chickens compared to the severe lesions observed in the unvaccinated control group.

Figure 2. Gross pathological changes observed during necropsy of chickens following FAdV-4 challenge. Representative gross lesions observed at necropsy in control and vaccinated chickens. (**A**,**B**) Control group: (**A**) liver showing marked enlargement, jaundice, and hemorrhagic foci associated with hydropericardium; (**B**) kidneys exhibiting enlargement and mottled appearance consistent with urate deposition. (**C**,**D**) 20 μg vaccinated group: (**C**) kidneys with normal size and appearance; (**D**) liver and heart showing no evident pathological alterations. (**E**,**F**) 10 μg vaccinated group: (**E**) liver and heart with mild congestion and minimal pericardial effusion; (**F**) kidneys with mild, focal discoloration. These images illustrate the marked reduction in gross pathological lesions in vaccinated groups compared with the unvaccinated control group, with the most pronounced protective effect observed in chickens receiving the 20 μg vaccine dose.

3.7.3. Score for Abnormalities Found in Different Organs

Postmortem examinations on chickens in the control group were promptly carried out, with organ lesions scored according to established criteria. For the immunized group, postmortem examinations were performed 14 days after challenge infection to document organ lesions, and the mean lesion scores for each organ across groups were calculated (Table 3). A summary bar graph comparing the average composite lesion scores across the heart, liver, spleen, and kidneys for the control, 10 μg, and 20 μg groups provides a clear visual representation of the dose-dependent reduction in gross pathology (Figure 3).

Briefly, results showed significant lesions in the heart, liver, spleen, and kidneys of the control group, with lesion scores of 6, 5.6, 4, and 5.8, respectively. Lesion scores for the pancreas and lungs were lower. Compared to the control group, lesion scores in all organs of the immunized group decreased, with lower lesion scores corresponding to higher immunization doses. In the 10 μg group, 80% of hearts and spleens showed lesions with scores of 0.8 and 1.4, respectively; 60% of livers exhibited lesions with a score of 1.4, while no gross lesions were observed in lungs. In the 20 μg group, 20% of hearts, livers, and kidneys showed lesions with lesion scores of 0.25, 0.5, and 0.375, respectively; 50% of spleens showed lesions with a lesion score of 0.625; and no gross lesions were observed in the lungs.

Table 3. Average gross lesion scores of major organs in chickens following FAdV-4 challenge.

	Heart	Liver	Spleen	Lungs	Kidneys	Pancreas
Control group (n = 10)	6 ± 0.82	5.6 ± 0.97	4 ± 1.15	0	5.8 ± 1.23	0.4 ± 0.7
10 µg group (n = 10)	0.8 ± 0.42 ***	1.4 ± 1.43 ***	1.4 ± 0.79 **	0	0.8 ± 0.42 **	0 *
20 µg group (n = 10)	0.25 ± 0.54 ***	0.5 ± 1.08 ***	0.625 ± 0.72 ***	0	0.375 ± 0.84 ***	0 *

Gross pathological lesions of the heart, liver, spleen, lungs, kidneys, and pancreas were scored in control and vaccinated chickens according to predefined criteria (0–10 scale) based on lesion severity. For the control group, scoring was performed at necropsy immediately after death. For vaccinated groups (10 µg and 20 µg), scoring was performed 14 days post-challenge. Data are expressed as mean lesion scores per organ. Statistical differences between vaccinated groups and the control group were analyzed using the Kruskal–Wallis test with Dunn's post hoc correction. * $p \leq 0.05$, ** $p \leq 0.01$, *** $p \leq 0.001$ indicate significant differences compared with the control group.

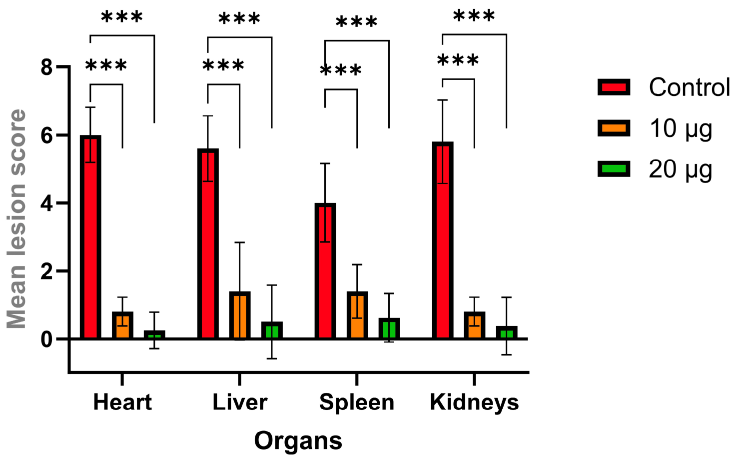

Figure 3. Dose-dependent reduction in gross pathological lesion scores following FAdV-4 challenge. Mean lesion scores (0–10 scale) for heart, liver, spleen, and kidneys in control (saline), 10 µg vaccinated, and 20 µg vaccinated chicken groups at 14 days post-challenge. Lesions were scored according to predefined criteria (0 = no lesions, 10 = severe lesions). Error bars represent standard deviation. Statistical significance compared to control group: *** $p \leq 0.001$ (Kruskal–Wallis test with Dunn's post hoc correction).

3.7.4. Histopathology and Immunohistochemical Findings

Histopathological examination revealed severe lesions in chickens from the control group, consistent with typical hydropericardium–hepatitis syndrome as previously described [5,24,25]. These included myocardial oedema, marked hepatocellular vacuolar degeneration and necrosis accompanied by intranuclear basophilic inclusion bodies, and renal tubular epithelial degeneration and necrosis (Figure 4). Immunohistochemical analysis demonstrated extensive FAdV-4 antigen expression in hepatocytes, renal tubular epithelial cells, and pancreatic acinar cells of control birds (Figure 5). All examined control animals were positive for viral antigen in the liver, kidney, and pancreas (Supplementary Table S2).

3.7.5. Distribution of the Virus in Different Organs

In the 10 µg vaccinated group, histopathological changes were clearly reduced in both frequency and severity. Myocardial oedema and hepatic vacuolar degeneration with focal necrosis were observed in a subset of birds, while renal lesions were mild and focal. Consistent with these findings, immunohistochemistry revealed scattered and weak FAdV-4 antigen labeling, primarily confined to the liver and pancreas, with no detectable antigen in the kidneys. Quantitative analysis confirmed that only 40% of birds in this group were

https://doi.org/10.3390/microbiolres17030048

positive for viral antigen in the liver and pancreas (Supplementary Table S2), and the overall frequency of histopathological lesions was significantly lower than in the control group (Supplementary Table S3).

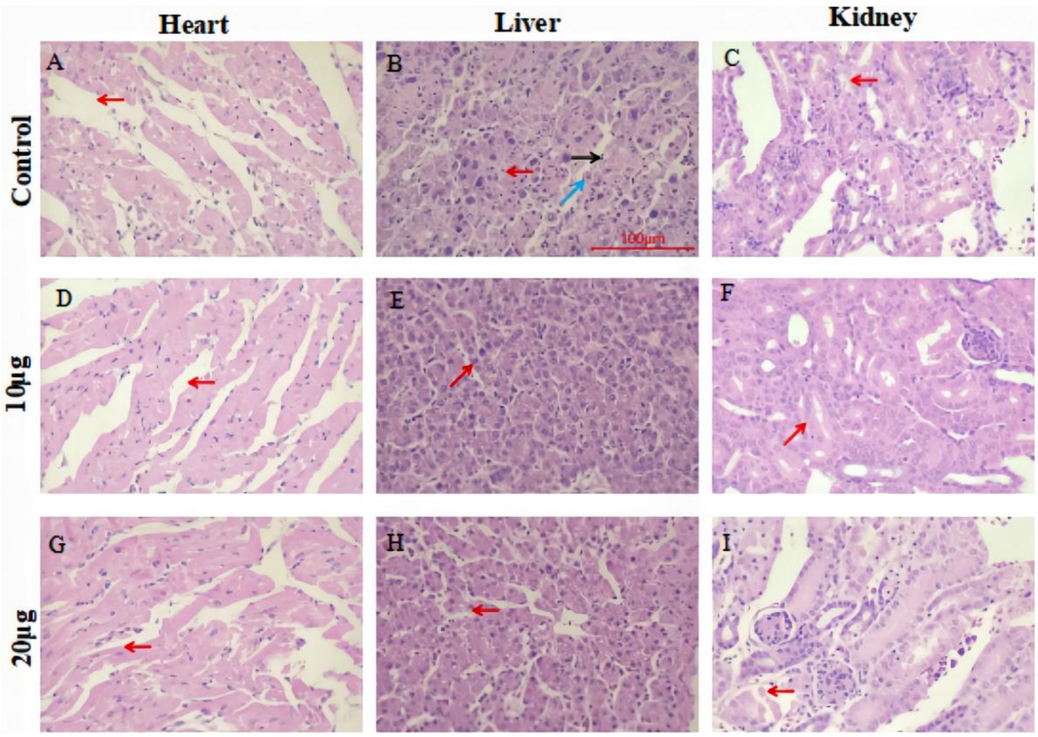

Figure 4. Histopathological changes in major organs of chickens following FAdV-4 challenge. (**A**–**C**) Control group: (**A**) heart showing marked myocardial oedema (red arrow); (**B**) hepatocytes exhibit basophilic inclusions within the nucleus (black arrow), vacuolar degeneration (blue arrow), and hepatocyte degeneration and necrosis (red arrow); (**C**) kidney showing tubular epithelial degeneration and necrosis with luminal desquamation (red arrow). (**D**–**F**) 10 μg vaccinated group: (**D**) heart with mild myocardial oedema (red arrow); (**E**) liver showing focal hepatocellular vacuolar degeneration and limited necrosis (red arrow); (**F**) kidney displaying mild tubular epithelial degeneration (red arrow). (**G**–**I**) 20 μg vaccinated group: (**G**) heart with preserved myocardial architecture and minimal oe-dema (red arrow); (**H**) liver showing occasional mild vacuolar degeneration without necrosis (red arrow); (**I**) kidney with normal tubular morphology and no evident pathological changes (red arrow).

In contrast, chickens immunized with the 20 μg dose exhibited minimal histopathological alterations. Occasional mild myocardial oedema and limited hepatocellular vacuolar degeneration were observed in a small proportion of birds, while no relevant renal or pancreatic lesions were detected. Importantly, immunohistochemical staining failed to detect FAdV-4 antigen in any examined organ from this group (Supplementary Table S2). The frequency of histopathological lesions was correspondingly low across all organs, indicating near-complete tissue-level protection (Supplementary Table S3).

Collectively, these findings demonstrate a clear dose-dependent reduction in both tissue damage and viral antigen distribution following vaccination, with the 20 μg bivalent *hexon-L1* and *fiber-2* formulation providing effective suppression of viral replication and associated pathological changes.

Randomly selected brains, hearts, lungs, livers, kidneys, and pancreases from 5 dead chickens of each different group were used for DNA extraction followed by PCR and electrophoresis. The viral DNA distribution analysis further elucidated the vaccine's efficacy in limiting systemic viral spread. This analysis confirmed markedly reduced viral loads in the organs of vaccinated chickens compared to the challenge control group in which viral DNA was detected in all examined organs (5/5) by PCR. Results showed that the virus was detected in all tissues and organs of the control group chickens. The pancreatic virus DNA detection rate was 60% in the 10 μg group, while virus was not detected in any organs of the 20 μg group (Table 4) under the conditions tested. A heatmap or stacked bar chart effectively visualizes this dose-dependent clearance of viral DNA from tissues, contrasting the widespread detection in controls with the restricted or absent detection in vaccinated groups (Figure 6).

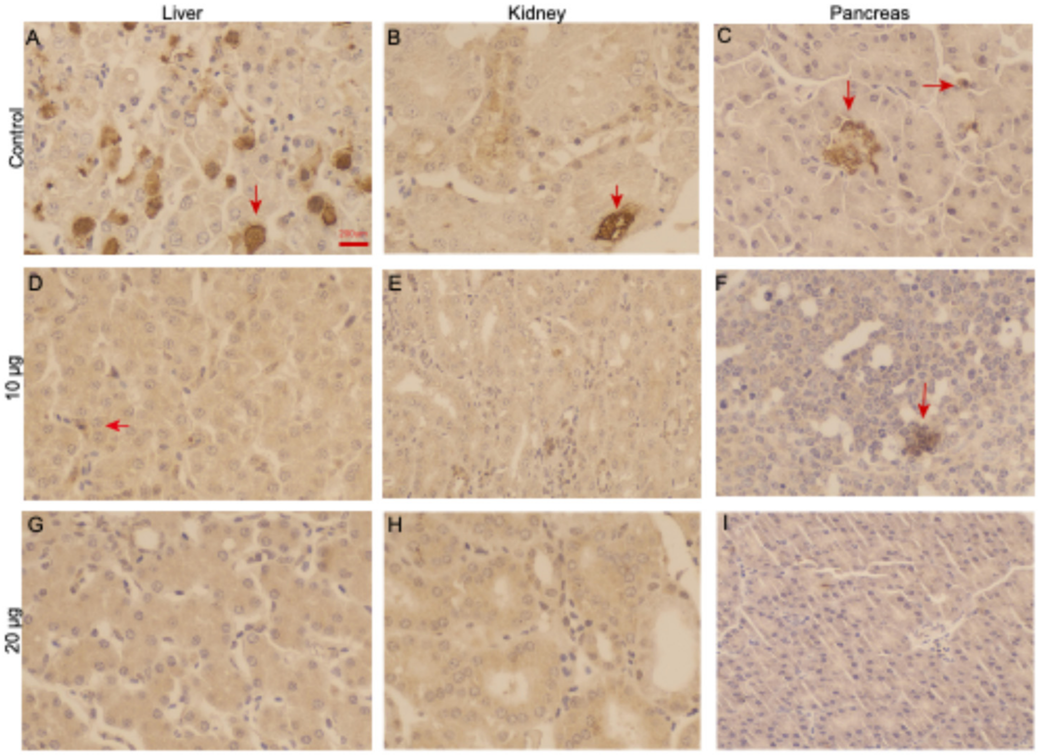

Figure 5. Immunohistochemical detection of FAdV-4 antigens in tissues of challenged chickens. Representative immunohistochemical staining of liver, kidney, and pancreas sections (100×) using an anti-FAdV-4-specific primary antibody. (**A**–**C**) Control group: strong positive immunoreactivity (brown staining indicated by red arrow) observed in hepatocytes (**A**), renal tubular epithelial cells (**B**), and pancreatic acinar cells (**C**), indicating extensive viral antigen distribution. (**D**–**F**) 10 μg vaccinated group: weak and scattered positive staining detected in the liver (**D**) and pancreas (**F**) (brown staining indicated by red arrow), with no detectable viral antigen in the kidney (**E**). (**G**–**I**) 20 μg vaccinated group: absence of detectable FAdV-4 antigen in the liver (**G**), kidney (**H**), and pancreas (**I**), indicating effective suppression of viral replication.

Table 4. Detection of FAdV-4 DNA in tissues of chickens at different time points after challenge.

	Heart	Liver	Kidney	Lungs	Pancreas	Brain
Control group	5/5	5/5	5/5	5/5	5/5	5/5
10 μg group	0/5	0/5	0/5	0/5	3/5	0/5
20 μg group	0/5	0/5	0/5	0/5	0/5	0/5

Viral DNA was detected by PCR in heart, liver, kidney, spleen, lungs, and pancreas samples collected from chickens in the control and vaccinated groups at 3, 5, 7, and 14 days post-infection (dpi). Results are expressed as number of PCR-positive organs per total examined organs. For the control group, tissue sampling was limited to time points prior to mortality. Vaccinated groups exhibited a dose-dependent reduction in viral tissue distribution, with no detectable viral DNA in any examined organ from chickens immunized with the 20 μg vaccine dose.

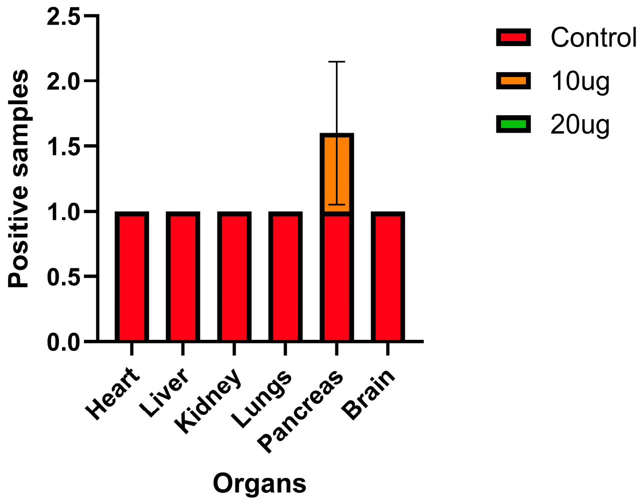

Figure 6. Heatmap of viral DNA detection in organs following FAdV-4 challenge. Tissues were collected from chickens in the control, 10 µg vaccinated, and 20 µg vaccinated groups at necropsy. Viral DNA was detected by PCR and results are expressed as the percentage of PCR-positive organs per group (n = 5 chickens per group). The control group showed 100% positivity in all organs, while the 10 µg group showed 60% positivity only in the pancreas. The 20 µg group showed no viral DNA detection in any organ.

3.7.6. Virus Shedding

After challenge, cloacal swabs were taken at 3, 5, 7 and 14 days post-infection from five randomly selected chickens from each group, and DNA was extracted, amplified by PCR and subjected to electrophoresis. The results showed that the control group had viral shedding from 3 dpi; the 10 µg group had a viral shedding rate of 40% at 3 dpi, 20% at 5 dpi, and no shedding at 7 or 14 dpi. The 20 µg group showed no viral shedding at any time (Table 5). The dynamics of viral shedding are clearly depicted in a line graph, showing the percentage of shedders over time for each group, highlighting the rapid and complete suppression of shedding in the 20 µg group (Figure 7).

Table 5. Detection of FAdV-4 shedding in cloacal swabs of chickens at different time points after challenge.

	3 dpi	5 dpi	7 dpi	14 dpi
Control group	5/5	-	-	-
10 µg group	2/5	1/5	0/5	0/5
20 µg group	0/5	0/5	0/5	0/5

Cloacal swabs were collected from five randomly selected chickens per group at 3, 5, 7, and 14 days post-infection (dpi) and analyzed by PCR for the presence of FAdV-4 DNA. Results are expressed as number of PCR-positive birds per total tested birds. No data are available for the control group beyond 5 dpi because all control birds died by that time point. Vaccination resulted in a dose-dependent reduction of viral shedding, with complete suppression observed in the 20 µg group.

3.7.7. Antibody Titers

Serum antibody titers were measured prior to each immunization. Prior to the first immunization, antibody titers were nearly identical in all three groups. After the first immunization, antibody titers increased in both the 10 µg and 20 µg groups, with the 20 µg group showing higher levels than the 10 µg group. After the second immunization, antibody titers in both the 10 µg and 20 µg groups showed a marked increase, with the 20 µg group reaching 44 ng/mL. This dose-dependent humoral immune response is graphically summarized in a bar chart showing mean antibody concentrations at pre-vaccination, post-primary, and post-booster time points (Figure 8).

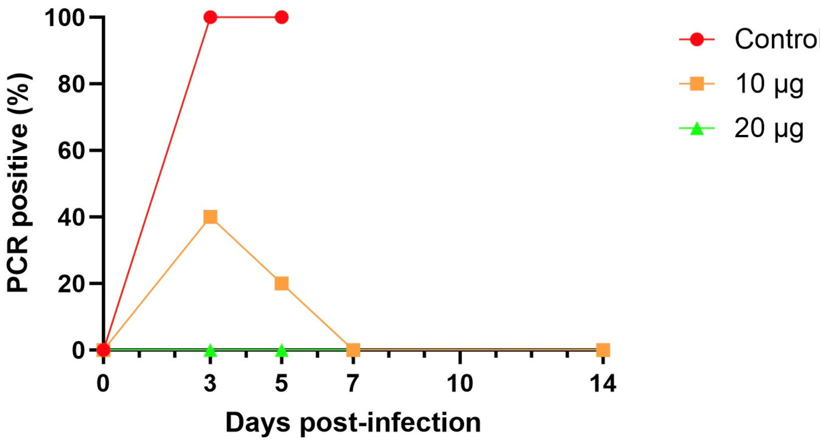

Figure 7. Dynamics of viral shedding in cloacal swabs following FAdV-4 challenge. Cloacal swabs were analyzed by PCR at 3, 5, 7, and 14 days post-infection. Results are expressed as the percentage of PCR-positive birds. The control group showed 100% shedding at 3 and 5 dpi (all birds died by 5 dpi). The 10 µg group showed reduced shedding over time (40% at 3 dpi, 20% at 5 dpi, and 0% thereafter). The 20 µg group showed no shedding at any time point.

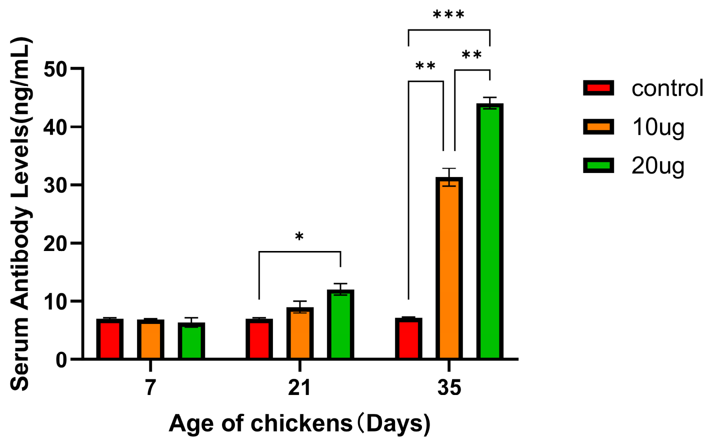

Figure 8. Serum antibody responses induced by the bivalent *hexon-L1* and *fiber-2* subunit vaccine. Mean serum antibody concentrations (ng/mL) measured by ELISA in chickens immunized with 10 µg or 20 µg of the bivalent subunit vaccine or saline (control). Serum samples were collected prior to primary immunization (day 0), two weeks after primary immunization (day 14), and two weeks after booster immunization (day 28, pre-challenge). Error bars represent standard deviation. The 20 µg group exhibited significantly higher antibody levels compared with the 10 µg group following booster immunization, indicating a dose-dependent humoral immune response. Statistical significance is indicated as * $p \leq 0.05$, ** $p \leq 0.01$, *** $p \leq 0.001$.

4. Discussion

Fowl adenovirus serotype 4 (FAdV-4) remains one of the most important viral pathogens affecting broiler chickens, particularly between 3 and 5 weeks of age, and is responsible for outbreaks of hydropericardium–hepatitis syndrome (HHS) associated with very high mortality rates and severe economic losses worldwide [24,25,29–34]. Despite the availability of inactivated and live-attenuated vaccines, control of HHS remains challenging due to incomplete protection, persistent viral shedding, and biosafety concerns [4,9,17,18]. In this context, subunit vaccines represent a safer alternative, as they exclude viral genomic material and eliminate risks related to incomplete inactivation or reversion to virulence [4,17].

The present study evaluated a bivalent subunit vaccine combining two major structural antigens of FAdV-4, *hexon-L1* and *fiber-2*, selected based on their established roles in antigenicity, virulence, and immune protection. *Fiber-2* has consistently been identified as the dominant protective antigen against HHS, inducing strong neutralizing antibody responses and high survival rates following challenge [19,20,35]. Genomic analyses have further demonstrated that *fiber-2* is a key virulence determinant, with most amino acid substitutions in hypervirulent strains clustering within the *fiber-2* and *hexon* regions [3,8]. Although *fiber-2*-based vaccines alone can provide substantial protection, previous studies have shown that protection may be incomplete under certain conditions, suggesting that inclusion of additional antigenic targets may enhance immune breadth and robustness.

In this work, recombinant *hexon-L1* and *fiber-2* proteins were successfully expressed in *Escherichia coli* and formulated into a water-in-oil bivalent vaccine. Following immunization and homologous challenge, both vaccine doses conferred significant protection compared with the control group, with a clear dose-dependent effect. Notably, the 20 μg dose provided complete protection against mortality, while the 10 μg dose resulted in partial protection with mild residual pathological changes. These findings are consistent with previous reports demonstrating that antigen dose is a critical determinant of protective efficacy in FAdV-4 subunit vaccines [20,35].

Serological analysis revealed a marked increase in antibody titers following booster immunization, particularly in the 20 μg group, indicating strong humoral immune activation. Although neutralizing antibodies were not directly measured, the observed dose-dependent reduction in viral tissue distribution and complete suppression of viral shedding in the 20 μg group strongly suggest that vaccine-induced antibodies played a central role in viral neutralization and clearance. This observation aligns with earlier studies reporting a close association between *fiber-2*-specific antibody responses and protection against HHS [19,35].

Pathological and histopathological findings further corroborated the protective efficacy of the bivalent vaccine. Control birds exhibited characteristic lesions of HHS, including myocardial oedema, hepatocellular vacuolar degeneration and necrosis with intranuclear inclusion bodies, and renal tubular damage. In contrast, vaccinated birds showed a marked reduction in lesion severity, with the 20 μg group displaying minimal or absent gross and microscopic lesions. Quantitative lesion scoring confirmed significantly lower scores across all examined organs in vaccinated groups, supporting the conclusion that vaccination effectively mitigated virus-induced tissue damage. These findings are consistent with other challenge studies demonstrating reduced pathological changes following effective vaccination against FAdV-4 [8,35,36].

Importantly, viral distribution and shedding analyses revealed a striking difference between groups. Viral DNA was detected in all examined tissues of control birds, whereas vaccinated birds showed a dose-dependent reduction in viral dissemination. While limited viral detection persisted in the pancreas of some birds in the 10 μg group, no viral DNA was detected in any organs or swab samples from the 20 μg group at any time point. Complete suppression of viral shedding is a particularly relevant outcome, as it suggests a reduced risk of environmental contamination and horizontal transmission within poultry flocks, a major limitation of many existing vaccines [9,12].

Collectively, these results demonstrate that the *hexon-L1* and *fiber-2* bivalent subunit vaccine induces strong, dose-dependent protective immunity against homologous FAdV-4 challenge. The complete protection observed at the 20 μg dose—characterized by absence of mortality, minimal pathology, and elimination of detectable virus—supports the feasibility of this bivalent strategy. While *fiber-2* has been established as a key protective antigen, the present study was not designed to evaluate whether inclusion of *hexon-L1* provides additional benefit over *fiber-2* alone. The observed protection reflects the combined effect of both antigens under the conditions tested, and no conclusions regarding additive or synergistic efficacy can be drawn in the absence of a *fiber*-2-only comparator group.

In conclusion, this study provides experimental evidence that a bivalent *hexon-L1* and *fiber-2* subunit vaccine can induce robust, dose-dependent protection against the homologous highly pathogenic FAdV-4 strain SDLC202009 isolated from our laboratory, effectively reducing mortality, pathological damage, viral dissemination, and shedding. These findings support further development and optimization of this vaccine candidate as a safe and effective strategy for the control of hydropericardium–hepatitis syndrome in poultry.

It is important to note that the protection efficacy demonstrated here is against the homologous challenge strain. Future studies are needed to evaluate the cross-protective potential of this vaccine candidate against other genetically or antigenically divergent FAdV-4 field strains.

4.1. Limitations of the Study

Several limitations of the present study should be acknowledged.

First, the sample size (n = 10 per group) was relatively small, and histological and immunohistochemical analyses were performed on tissues from five randomly selected animals per group. While the data obtained indicate that the bivalent subunit vaccine induces protective immunity, larger studies with $\geq$50 birds per group are recommended to confirm statistical power and assess commercial relevance.

Second, a major limitation is the absence of a *fiber-2*-only vaccinated control group. As *fiber-2* has previously been shown to confer high levels of protection against FAdV-4 challenge [19,20,35], the current experimental design does not allow direct assessment of whether inclusion of *hexon-L1* provides additive or synergistic benefit. Consequently, conclusions regarding superiority over monovalent *fiber-2* vaccination cannot be drawn from this study. Future work should include comparative challenge experiments using *fiber-2*-only, *hexon-L1*-only, and bivalent formulations to clarify the precise contribution of each antigen.

Third, protection was demonstrated only against the homologous challenge strain (SDLC202009). The cross-protective potential of this vaccine candidate against other genetically or antigenically divergent FAdV-4 field strains remains to be evaluated.

Fourth, while ELISA-detected antibody responses were measured, neutralizing antibody titers were not assessed. As antibodies detected by ELISA do not fully correspond to neutralizing capacity, the analysis of protective mechanisms remains incomplete. Future studies should include virus neutralization assays to better characterize functional immune responses.

Fifth, the study evaluated protection only at 14 days post-challenge; long-term immunity, cellular immune responses, mucosal immunity, and efficacy under field conditions were not assessed. The duration of protective immunity and the potential for memory responses require further investigation.

Despite these limitations, the complete absence of virus shedding in the 20 μg group is a promising result, suggesting that the vaccine may help reduce environmental contamination and horizontal transmission in poultry flocks.

Overall, the study provides experimental evidence supporting the immunogenicity and protective efficacy of the bivalent *hexon-L1* + *fiber-2* formulation against homologous challenge. Future studies incorporating monovalent *fiber-2* and *hexon-L1* control groups will be necessary to determine the specific contribution of each antigen to the observed protection.

4.2. Future Research Directions

Further research involving larger cohorts, extended observation periods, and field trials is imperative to validate these preliminary findings and assess the vaccine's efficacy under diverse environmental and challenge conditions. Given that *fiber-2* alone has produced up to 100% protection in prior studies [8,19,35], future work must include comparative arms with monovalent *fiber-2* and *hexon-L1* vaccines to determine whether the bivalent formulation provides any additive benefit. Additionally, evaluation of cross-protection against heterologous FAdV-4 strains, assessment of neutralizing antibody responses, and characterization of cell-mediated immunity will be essential to fully define the immunological mechanisms and practical relevance of this vaccine candidate in poultry production.

5. Conclusions

The bivalent *hexon-L1* and *fiber-2* subunit vaccine developed in this study exhibited strong immunogenicity and conferred effective, dose-dependent protection against homologous FAdV-4 challenge in SPF chickens. Vaccinated birds showed complete survival, markedly reduced pathological lesions, and substantial suppression of viral replication, tissue distribution, and shedding, particularly at the 20 μg antigen dose. These results indicate that the proposed bivalent formulation represents a feasible and promising subunit vaccine approach for the prevention of hydropericardium-hepatitis syndrome.

Although the higher antigen dose resulted in more consistent protection, the present study was not designed to determine the specific contribution of *hexon-L1* relative to *fiber-2* alone. Therefore, conclusions regarding additive or synergistic efficacy cannot be drawn. Comparative evaluations including monovalent *fiber-2* vaccines are essential to define the precise immunological role of each antigen. Future studies involving larger cohorts, alternative routes of administration, and formulations with or without adjuvants will be necessary to further validate immunogenicity and protective capacity. In addition, comparative evaluations including monovalent *fiber-2* vaccines, commercially available products, and long-term immunity assessments will be essential to define the practical and epidemiological relevance of this vaccine candidate in poultry production.

Overall, this study provides experimental evidence supporting the feasibility of a bivalent *hexon-L1* and *fiber-2* subunit vaccine and establishes a solid foundation for the rational development of safer and effective vaccination strategies to control hydropericardium-hepatitis syndrome in poultry.

Supplementary Materials: The following are available online at: https://www.mdpi.com/article/10.3390/microbiolres17030048/s1, Table S1: Description of the two primary forms of virulence based on the clinical presentation of the disease and pathophysiological dominance; Table S2: Frequency of FAdV-4 antigen detection by immunohistochemistry (IHC) in different organs after challenge; Table S3. Frequency of histopathological lesions observed in different organs of chickens following FAdV-4 challenge; Figure S1: PCR amplification of *hexon-L1* and ***fiber-2*** gene fragments from FAdV-4 genomic DNA; Figure S2: Colony PCR screening for recombinant *pET-32a(+)-hexon-L1* plasmids; Figure S3: Colony PCR screening for recombinant *pET-32a(+)-fiber-2* plasmids; Figure S4: Restriction enzyme digestion analysis of recombinant expression plasmids; Figure S5: Optimization of recombinant *hexon-L1* protein expression in ***E. coli*** Rosetta (DE3); Figure S6: Analysis of recombinant ***fiber-2*** protein expression in ***E. coli*** Rosetta (DE3) at 37 °C; Figure S7: Comprehensive optimization of recombinant ***fiber-2*** expression parameters; Figure S8: Purification of recombinant *hexon-L1* and ***fiber-2*** proteins by Ni-NTA affinity chromatography.

Author Contributions: Conceptualization, Z.S. and Y.L.; methodology, X.C. and K.W.; formal analysis, X.C., C.L. and K.W.; investigation, X.C., C.L. and K.W.; data curation, X.C., C.L. and K.W.; writing—original draft preparation, X.C. and K.W.; writing—review and editing, V.C. and Z.S.; supervision, Y.L. All authors have read and agreed to the published version of the manuscript.

Funding: This work was supported by the Key R&D Program of Shandong Province [number 2022CXGC010606], the Key R&D Program of Shandong Province (Public Welfare) [number

2019GNC106082], the Shandong Natural Science Foundation [number ZR2020MC175], Doctoral research Foundation of Liaocheng University [number 318052237].

Institutional Review Board Statement: The animal study protocol was approved by the Ethics Committee of the Research Ethics Committee of Liaocheng University (protocol code 2022092001 and date of approval 20 September 2022).

Data Availability Statement: The raw data supporting the conclusions of this article will be made available by the authors on request.

Conflicts of Interest: The authors declare no conflicts of interest.

References

1. Benkő, M.; Aoki, K.; Arnberg, N.; Davison, A.J.; Echavarría, M.; Hess, M.; Jones, M.S.; Kaján, G.L.; Kajon, A.E.; Mittal, S.K.; et al. ICTV Virus Taxonomy Profile: Adenoviridae 2022. *J. Gen. Virol.* **2022**, *103*, 001721. [CrossRef] [PubMed]
2. Marek, A.; Günes, A.; Schulz, E.; Hess, M. Classification of fowl adenoviruses by use of phylogenetic analysis and high-resolution melting-curve analysis of the hexon L1 gene region. *J. Virol. Methods* **2010**, *170*, 147–154. [CrossRef] [PubMed]
3. Liu, Y.; Wan, W.; Gao, D.; Li, Y.; Yang, X.; Liu, H.; Yao, H.; Chen, L.; Wang, C.; Zhao, J. Genetic characterization of novel fowl aviadenovirus 4 isolates from outbreaks of hepatitis-hydropericardium syndrome in broiler chickens in China. *Emerg. Microbes Infect.* **2016**, *5*, e117. [CrossRef]
4. Liu, A.; Zhang, Y.; Cui, H.; Wang, X.; Gao, Y.; Pan, Q. Advances in Vaccine Development of the Emerging Novel Genotype Fowl Adenovirus 4. *Front. Immunol.* **2022**, *13*, 916290. [CrossRef]
5. Niu, Y.; Sun, Q.; Zhang, G.; Sun, W.; Liu, X.; Xiao, Y.; Shang, Y.; Liu, S. Pathogenesis of Hypervirulent Fowl Adenovirus Serotype 4: The Contributions of Viral and Host Factors. *Viruses* **2020**, *12*, 741. [CrossRef]
6. Mu, Y.; Xie, Q.; Wang, W.; Lu, H.; Lian, M.; Gao, W.; Li, T.; Wan, Z.; Shao, H.; Qin, A.; et al. A Novel Fiber-1-Edited and Highly Attenuated Recombinant Serotype 4 Fowl Adenovirus Confers Efficient Protection Against Lethal Challenge. *Front. Vet. Sci.* **2021**, *8*, 759418. [CrossRef]
7. Wang, K.; Liu, C.; Du, X.; Ma, Y.; Chen, L.; Cao, S.; Lu, J.; Li, Y.; Si, Z. Complete genome sequence and pathogenicity analysis of a highly pathogenic FAdV-4 strain. *Res Vet. Sci.* **2023**, *159*, 84–92. [CrossRef]
8. Xie, Q.; Wang, W.; Kan, Q.; Mu, Y.; Zhang, W.; Chen, J.; Li, L.; Fu, H.; Li, T.; Wan, Z.; et al. FAdV-4 without Fiber-2 Is a Highly Attenuated and Protective Vaccine Candidate. *Microbiol. Spectr.* **2022**, *10*, e0143621. [CrossRef]
9. Li, L.; Wang, J.; Chen, P.; Zhang, S.; Sun, J.; Yuan, W. Pathogenicity and molecular characterization of a fowl adenovirus 4 isolated from chicken associated with IBH and HPS in China. *BMC Vet. Res.* **2018**, *14*, 400. [CrossRef]
10. San Martín, C. Latest insights on adenovirus structure and assembly. *Viruses* **2012**, *4*, 847–877. [CrossRef] [PubMed]
11. Pan, Q.; Zhang, Y.; Liu, A.; Cui, H.; Gao, Y.; Qi, X.; Liu, C.; Zhang, Y.; Li, K.; Gao, L.; et al. Development of a Novel Avian Vaccine Vector Derived from the Emerging Fowl Adenovirus 4. *Front. Microbiol.* **2021**, *12*, 780978. [CrossRef]
12. Chen, H.; Dou, Y.; Zheng, X.; Tang, Y.; Zhang, M.; Zhang, Y.; Wang, Z.; Diao, Y. Hydropericardium Hepatitis Syndrome Emerged in Cherry Valley Ducks in China. *Transbound. Emerg. Dis.* **2017**, *64*, 1262–1267. [CrossRef]
13. El-Shall, N.A.; El-Hamid, H.S.A.; Elkady, M.F.; Ellakany, H.F.; Elbestawy, A.R.; Gado, A.R.; Geneedy, A.M.; Hasan, M.E.; Jaremko, M.; Selim, S.; et al. Corrigendum: Epidemiology, pathology, prevention, and control strategies of inclusion body hepatitis and hepatitis-hydropericardium syndrome in poultry: A comprehensive review. *Front. Vet. Sci.* **2022**, *9*, 1075948. [CrossRef] [PubMed]
14. Rashid, F.; Xie, Z.; Wei, Y.; Xie, Z.; Xie, L.; Li, M.; Luo, S. Biological features of fowl adenovirus serotype-4. *Front. Cell Infect. Microbiol.* **2024**, *14*, 1370414. [CrossRef] [PubMed]
15. Liu, X.N.; Guo, X.R.; Han, Y.; Tian, T.; Sun, J.; Lei, B.S.; Zhang, W.C.; Yuan, W.Z.; Zhao, K. The Cellular and Viral circRNAs Induced by Fowl Adenovirus Serotype 4 Infection. *Front. Microbiol.* **2022**, *13*, 925953. [CrossRef]
16. Schachner, A.; Marek, A.; Jaskulska, B.; Bilic, I.; Hess, M. Recombinant FAdV-4 fiber-2 protein protects chickens against hepatitis-hydropericardium syndrome (HHS). *Vaccine* **2014**, *32*, 1086–1092. [CrossRef] [PubMed]
17. Wang, X.; Tang, Q.; Chu, Z.; Wang, P.; Luo, C.; Zhang, Y.; Fang, X.; Qiu, L.; Dang, R.; Yang, Z. Immune protection efficacy of FAdV-4 surface proteins fiber-1, fiber-2, hexon and penton base. *Virus Res.* **2018**, *245*, 1–6. [CrossRef]
18. Toogood, C.I.; Crompton, J.; Hay, R.T. Antipeptide antisera define neutralizing epitopes on the adenovirus hexon. *J. Gen. Virol.* **1992**, *73*, 1429–1435. [CrossRef]
19. Fang, C.M.; Zainuddin, Z.F.; Musa, M.; Thong, K.L. Cloning, expression, and purification of recombinant protein from a single synthetic multivalent construct of Mycobacterium tuberculosis. *Protein Expr. Purif.* **2006**, *47*, 341–347. [CrossRef]
20. Behloul, N.; Baha, S.; Liu, Z.; Wei, W.; Zhu, Y.; Rao, Y.; Shi, R.; Meng, J. Design and development of a chimeric vaccine candidate against zoonotic hepatitis E and foot-and-mouth disease. *Microb. Cell Fact.* **2020**, *19*, 137. [CrossRef]

21. Landmann, M.; Scheibner, D.; Graaf, A.; Gischke, M.; Koethe, S.; Fatola, O.I.; Raddatz, B.; Mettenleiter, T.C.; Beer, M.; Grund, C.; et al. A Semiquantitative Scoring System for Histopathological and Immunohistochemical Assessment of Lesions and Tissue Tropism in Avian Influenza. *Viruses* **2021**, *13*, 868. [CrossRef]
22. Bertran, K.; Pantin-Jackwood, M.J.; Criado, M.F.; Lee, D.H.; Balzli, C.L.; Spackman, E.; Suarez, D.L.; Swayne, D.E. Pathobiology and innate immune responses of gallinaceous poultry to clade 2.3.4.4A H5Nx highly pathogenic avian influenza virus infection. *Vet. Res.* **2019**, *50*, 89. [CrossRef] [PubMed]
23. Sánchez-González, R.; Ramis, A.; Nofrarías, M.; Wali, N.; Valle, R.; Pérez, M.; Perlas, A.; Majó, N. Pathobiology of the highly pathogenic avian influenza viruses H7N1 and H5N8 in different chicken breeds and role of Mx 2032 G/A polymorphism in infection outcome. *Vet. Res.* **2020**, *51*, 113. [CrossRef] [PubMed]
24. Ma, H.; Ding, Y.; Du, K.; Chang, K.; Niu, Y. FAdV-4 induce autophagy via the endoplasmic reticulum stress-related unfolded protein response. *Vet. Microbiol.* **2022**, *269*, 109388. [CrossRef] [PubMed]
25. Abe, T.; Nakamura, K.; Tojo, H.; Mase, M.; Shibahara, T.; Yamaguchi, S.; Yuasa, N. Histology, immunohistochemistry, and ultrastructure of hydropericardium syndrome in adult broiler breeders and broiler chicks. *Avian Dis.* **1998**, *42*, 606–612. [CrossRef]
26. Mase, M.; Hiramatsu, K.; Nishijima, N.; Iguchi, H.; Honda, S.; Hanyu, S.; Iseki, H.; Watanabe, S. Fowl Adenoviruses Type 8b Isolated from Chickens with Inclusion Body Hepatitis in Japan. *Avian Dis.* **2020**, *64*, 330–334. [CrossRef]
27. Kim, J.N.; Byun, S.H.; Kim, M.J.; Kim, J.; Sung, H.W.; Mo, I.P. Outbreaks of hydropericardium syndrome and molecular characterization of Korean fowl adenoviral isolates. *Avian Dis.* **2008**, *52*, 526–530. [CrossRef]
28. Choi, K.S.; Kye, S.J.; Kim, J.Y.; Jeon, W.J.; Lee, E.K.; Park, K.Y.; Sung, H.W. Epidemiological investigation of outbreaks of fowl adenovirus infection in commercial chickens in Korea. *Poult. Sci.* **2012**, *91*, 2502–2506. [CrossRef]
29. Asrani, R.K.; Gupta, V.K.; Sharma, S.K.; Singh, S.P.; Katoch, R.C. Hydropericardium-hepatopathy syndrome in Asian poultry. *Vet. Rec.* **1997**, *141*, 271–273. [CrossRef]
30. Dahiya, S.; Srivastava, R.N.; Hess, M.; Gulati, B.R. Fowl adenovirus serotype 4 associated with outbreaks of infectious hydropericardium in Haryana, India. *Avian Dis.* **2002**, *46*, 230–233. [CrossRef]
31. Ye, J.; Liang, G.; Zhang, J.; Wang, W.; Song, N.; Wang, P.; Zheng, W.; Xie, Q.; Shao, H.; Wan, Z.; et al. Outbreaks of serotype 4 fowl adenovirus with novel genotype, China. *Emerg. Microbes Infect.* **2016**, *5*, e50. [CrossRef] [PubMed]
32. Zhu, C.; Yang, P.; Zhou, J.; Liu, X.; Huang, Y.; Wan, C. Advances and Prospects of Fowl Adenoviruses Vaccine Technologies in the Past Decade. *Int. J. Mol. Sci.* **2025**, *26*, 6434. [CrossRef] [PubMed]
33. Zhang, Y.; Liu, R.; Tian, K.; Wang, Z.; Yang, X.; Gao, D.; Zhang, Y.; Fu, J.; Wang, H.; Zhao, J. Fiber2 and hexon genes are closely associated with the virulence of the emerging and highly pathogenic fowl adenovirus 4. *Emerg. Microbes Infect.* **2018**, *7*, 199. [CrossRef] [PubMed]
34. Yin, D.; He, L.; Zhu, E.; Fang, T.; Yue, J.; Wen, M.; Wang, K.; Cheng, Z. A fowl adenovirus serotype 4 (FAdV-4) Fiber2 subunit vaccine candidate provides complete protection against challenge with virulent FAdV-4 strain in chickens. *Vet. Microbiol.* **2021**, *263*, 109250. [CrossRef]
35. De Luca, C.; Schachner, A.; Mitra, T.; Heidl, S.; Liebhart, D.; Hess, M. Fowl adenovirus (FAdV) fiber-based vaccine against inclusion body hepatitis (IBH) provides type-specific protection guided by humoral immunity and regulation of B and T cell response. *Vet. Res.* **2020**, *51*, 143. [CrossRef]
36. Ali, S.; Mahmood, S.; Hussain, I.; Khan, M. Preparation and Evaluation of Lyophilized Live Attenuated Vaccine of Inclusion Body Hepatitis Hydropericardium Syndrome (IBH-HPS) against Challenge in Broiler Chickens. *Int. J. Agric. Biol.* **2015**, *17*, 658–662. [CrossRef]

https://doi.org/10.3390/microbiolres17030048